Drive of a long-lived vortex-flow pattern by coupling to zonal flows in presence of resonant magnetic perturbations

M. Leconte and J.-H. Kim

Citation: Physics of Plasmas **22**, 082301 (2015); doi: 10.1063/1.4927776
View online: http://dx.doi.org/10.1063/1.4927776
View Table of Contents: http://scitation.aip.org/content/aip/journal/pop/22/8?ver=pdfcov
Published by the AIP Publishing

Drive of a long-lived vortex-flow pattern by coupling to zonal flows in presence of resonant magnetic perturbations

M. Leconte[a] and J.-H. Kim
Advanced Physics Research Division, NFRI, Daejeon, South Korea

(Received 7 April 2015; accepted 10 July 2015; published online 5 August 2015)

The working hypothesis for the origin of edge-localized-mode stabilization is that Resonant Magnetic Perturbations (RMPs) increase transport in the pedestal, thus lowering the pressure gradient below the ideal MHD threshold. Large-scale vortex-flows matching the RMP helicity were observed experimentally [N. Vianello *et al.*, Plasma Phys. Controlled Fusion **57**, 014027 (2015)]. We derive and solve numerically a 1D model for the generation of long-lived vortex-flows in presence of RMPs. We show that, in presence of RMPs, zonal flows are damped and partially transfer their energy to a resonant vortex-flow pattern. The resulting vortex-flow has a multiscale nature with a fast-varying fine-structure set by zonal flows and a slowly-varying radial envelope with a resonant character. The model predicts that the saturated vortex-flow energy E scales with RMP amplitude as $E \sim \frac{\delta B_r}{B}^{\alpha}$ with $\alpha \simeq 1.9$. This novel type of nonlinearly driven non-axisymmetric flow has a radial—streamer like—component, and is therefore a candidate for increased convective transport. © *2015 AIP Publishing LLC*. [http://dx.doi.org/10.1063/1.4927776]

I. INTRODUCTION

Self-organization is one of the most spread characteristics of non-linear systems in nature. In geophysical fluids and in solar physics, large-scale flows play a dominant role in this self-organization. Such flows are usually highly anisotropic, typically having a high degree of symmetry. In fusion devices, such flows known as Zonal Flows (ZFs) play a crucial role in attaining enhanced confinement regimes such as the H-mode. For a review, see, e.g., Ref. 1. In typical discharges, the H-mode—the target regime for next step fusion devices such as ITER—relaxes quasiperiodically, thus expelling large fluxes of heat and particles, an event called Edge Localized Mode (ELM). Controlling ELMs is thus very important for ITER, and a well-tested way to achieve this is by using external coils to generate Resonant Magnetic Perturbations (RMPs), demonstrated on several tokamaks.[2–5] The working hypothesis for the origin of ELM stabilization is that RMPs increase transport in the pedestal, thus lowering the pressure gradient below the ideal MHD threshold. Changes in turbulent transport during application of RMPs were observed in DIII-D.[6] In the latter reference, a fast increase in density fluctuations—measured using beam emission spectroscopy—was observed in the outer radial region, when RMPs were turned on. This change is faster than could be caused by the change in the equilibrium radial electric field. A possible candidate to explain this turbulence change is associated to damping of zonal flows.[7] Note that zonal flow damping by RMPs were first observed in 3D global fluid simulations.[8] Experimentally, damping of GAM zonal flows during RMP was observed in TEXTOR.[9] Non-axisymmetric convection cells associated to stationary large scale vortex flow (VF) patterns are another possible candidate for the observed transport increase in presence of RMPs, as was observed in 3D turbulence simulations of resistive ballooning mode turbulence (Fig. 11 of Ref. 10). Such large-scale vortex-flows matching the RMP helicity were observed experimentally.[11] In Ref. 12, it was shown that—when microturbulence is present—the tearing-parity equilibrium without zonal flows in presence of RMPs is unstable and a bifurcation to a new equilibrium with non-vanishing zonal flows was observed in turbulence simulations. In Ref. 13, it was pointed out that zonal flow damping is a resonant phenomenon, as it involves so-called Magnetostatic Cells (MCs). These MCs are actually a type of vortex-flow pattern *localized* around the resonance surface. In this article, we show that zonal flows can linearly couple to a long-lived vortex-flow pattern in presence of RMPs, and thus transfer energy to the latter, which results in enhanced ZF damping. The article is organized as follows: In Section II, we derive the model; in Section III, we solve the model numerically and describe numerical results; and in Section IV, we discuss the results, and finally, we give conclusions.

II. MODEL

We consider charge balance, in presence of RMPs

$$\rho_s^2 \frac{\partial}{\partial t}\frac{\partial^2 \phi}{\partial x^2} + \rho_s^2 \{\phi, \nabla_\perp^2 \phi\} = \nabla_\parallel j_\parallel, \tag{1}$$

where ρ_s is the sound gyroradius and $\{\phi, \cdot\} = \partial_x \phi \partial_y - \partial_y \phi \partial_x$ denote Poisson brackets, together with Ohm's law, which can be written as

$$j_\parallel = -D_\parallel \nabla_\parallel \phi, \tag{2}$$

$$= -D_\parallel \nabla_{\parallel 0} \phi + \delta b_x \frac{\partial \phi}{\partial x}, \tag{3}$$

where we use $|\frac{\partial}{\partial y}| \ll |\frac{\partial}{\partial x}|$ since we focus on low-k_y modes—except in the nonlinear term—and we neglect two-fluid effects in order to simplify the analysis. Here, $D_\parallel = v_{th,e}^2 \nu_{ei}^{-1}$ is the

[a]Email: mleconte@nfri.re.kr

parallel electron diffusivity, with $v_{th,e}$ the electron thermal speed and ν_{ei} the electron-ion collision frequency, and $\nabla_\parallel \sim \nabla_{\parallel 0} + \delta b_x \frac{\partial}{\partial x}$ is the perturbed parallel gradient, in the uniform-psi approximation. We assume a *coherent* form for the RMP magnetic field, i.e.

$$\delta b_x = \hat{b}_x \sin(K_y y), \tag{4}$$

where $y = r_s(\theta - \frac{N}{M}\varphi)$ is a field-aligned coordinate aligned along the *unperturbed* magnetic field. Here, N is the toroidal wavenumber of RMPs, K_y is the poloidal wavenumber at a particular resonance surface ($K_y = M/r_s$), and $\hat{b}_x > 0$ is the real-value amplitude, considering RMPs with a base mode $M:N$.

We now proceed to obtain coupled equations for vortex-flow and zonal flows.

(i) Flux-surface averaging Eq. (1) and adding a neoclassical ZF damping ($\mu \sim \nu_{ii}$), we obtain the evolution of ZFs coupled to $\hat{\phi}$. (ii) Taking the K_y cosine component of Eq. (1), multiplying it by $\cos(K_y y)$, and flux-surface averaging over unperturbed flux-surfaces, we obtain the evolution equation for $\hat{\phi}$ coupled to ZFs, where $\hat{\phi}$ is associated to the vortex-flow stream-function, and defined as

$$\hat{\phi}(x,t) = \langle \phi \cos(K_y y) \rangle. \tag{5}$$

After some algebra, we obtain the following 1D ZF-VF model:

$$\left[\frac{\partial}{\partial t} + \mu + \frac{1}{2}\frac{D_\parallel \hat{b}_x^2}{\rho_s^2}\right] V_{ZF} - \frac{1}{2}\frac{D_\parallel K_y}{\rho_s L_s}\hat{b}_x x \hat{\phi} = -\frac{\partial}{\partial x}\left(\nu_{UG}\frac{\partial V_{ZF}}{\partial x}\right), \tag{6}$$

$$\left[\rho_s^2 \frac{\partial}{\partial t}\frac{\partial^2}{\partial x^2} - \frac{D_\parallel K_y^2}{L_s^2}x^2\right]\hat{\phi} + \frac{D_\parallel K_y}{\rho_s L_s}\hat{b}_x x V_{ZF} = \rho_s^2 \nu_\perp^{diss}\frac{\partial^4 \hat{\phi}}{\partial x^4}, \tag{7}$$

where we included neoclassical friction (μ) for zonal flows, and viscous dissipation for the vortex-flow pattern. Here, $V_{ZF} = \rho_s \frac{\partial}{\partial x}\phi_{zon}$, and $\nu_{UG} > 0$ denotes an effective eddy viscosity due to turbulence, associated to up-gradient diffusion, i.e., the ZF nonlinear drive.

Equations (6) and (7) show that—in presence of RMPs—a vortex-flow pattern can be non-linearly driven. RMP effect can be understood from two points of view:

(i) From the point of view of zonal flows, Eq. (6) shows that RMPs render radial modes—i.e., zonal flows—vulnerable to *field-line bending*, effectively damping ZFs. In other words, ZFs *lose* energy via RMP coupling. Near the resonance surface $x = 0$, the relative enhancement in ZF damping—for large neoclassical ZF damping—as derived in Ref. 7 is given by

$$\frac{\Delta\gamma_d^{ZF}}{\gamma_{d0}^{ZF}} \sim \frac{D_\parallel \hat{b}_x^2}{\rho_s^2 \mu} = \frac{\mu_{RMP}}{\mu}. \tag{8}$$

(ii) However, from the point of view of the vortex-flow pattern, the vortex-flow *gains* energy via RMP coupling.

Hence, RMPs are shown to partially *transfer* energy from zonal flows to the vortex-flow, thus driving the latter, since zonal flows are ultimately non-linearly driven by turbulence. A schematic diagram of the interaction among turbulence, zonal flows, RMPs, and the vortex-flow pattern is shown [Fig. 1].

At this point, we wish to clarify the connection between our analysis and the concept of $j \times b$ torque. For this purpose, we may rewrite the charge balance equation (7) in the form

$$\rho_s^2 \frac{\partial}{\partial t}\frac{\partial^2 \hat{\phi}}{\partial x^2} - \rho_s^2 \nu_\perp^{diss}\frac{\partial^4 \hat{\phi}}{\partial x^4} = K_{\parallel 0}(x)\hat{j}_\parallel, \tag{9}$$

where $K_{\parallel 0}(x)$ is the unperturbed parallel wavenumber given by

$$K_{\parallel 0}(x) = -\frac{K_y x}{L_s}, \tag{10}$$

and the quantity $\hat{j}_\parallel$ is defined as

$$\hat{j}_\parallel = \langle j_\parallel \sin(K_y y) \rangle. \tag{11}$$

Using Ohm's law, the latter verifies

$$\hat{j}_\parallel = -D_\parallel [\hat{b}_x V_{ZF} + K_{\parallel 0}(x)\hat{\phi}]. \tag{12}$$

The related flux $\hat{b}_x \hat{j}_\parallel$ is associated to the $j \times b$ torque in tearing-mode theory. Since $\hat{j}_\parallel$ is clearly associated to the polarization charge of the vortex-flow pattern, we may call the associated torque $\hat{b}_x \hat{j}_\parallel$ as "polarization torque." This polarization torque should be *self-consistently* determined by the system formed by Eqs. (6), (9), and (12), which leads to the system (6, 7).

A. 1D ZF-VF model

1. Cahn-Hilliard model for zonal flow shear

Since the simple zonal flow evolution equation (6) does not have well-behaved solutions at large time, we model unperturbed ZF evolution ($\hat{b}_x = 0$) by a higher-order nonlinear equation, namely, a Cahn-Hilliard equation, known to generate jet-like flow patterns[14]

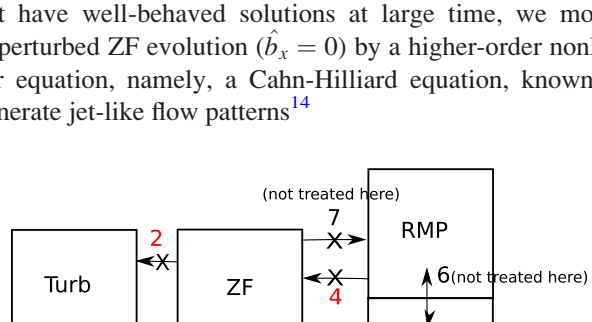

FIG. 1. Schematics of the interaction between turbulence, Zonal Flows (ZF), the Vortex Flow pattern (VF), and RMPs. The interactions are numbered as: 1. Reynolds-stress drive, 2. suppression by shearing, 3. drive by $\delta\mathbf{j} \times \mathbf{B}$ torque, 4. damping by $\langle \delta\mathbf{j} \times \delta\mathbf{b} \rangle$ torque, 5. drive and shearing between turbulence and Vortex-Flow, 6. plasma response, and 7. RMP screening. The physics of 5, 6, and 7 is not treated in the present model.

$$\frac{\partial V'_{ZF}}{\partial t} = -\frac{\partial^2}{\partial x^2}\left[\nu_{UG0}\left(V'_{ZF} - V'^3_{ZF}\right) + \nu_{hyp}\frac{\partial^2 V'_{ZF}}{\partial x^2}\right] - \mu V'_{ZF}, \tag{13}$$

with $V'_{ZF} = \partial_x V_{ZF}$ the zonal flow *shear* and where we introduced a hyper-viscosity (ν_{hyp}), and we modeled the turbulence-induced effective eddy viscosity as

$$\nu_{UG} = \nu_{UG0}[1 - V'^2_{ZF}], \tag{14}$$

with the second term in the bracket representing the stabilizing effect of ZF shearing on turbulent eddies. To our knowledge, this form of Cahn-Hillard model has never been applied to a plasma. By comparing Eq. (13) with the Cahn-Hilliard equation, the effective eddy diffusivity has the following analog:

$$\nu_{UG0} \sim \left[\frac{\gamma}{\gamma_c} - 1\right] \leftrightarrow m\left[\frac{T}{T_c} - 1\right], \tag{15}$$

with m the mobility in the original Cahn-Hilliard equation. In our model, the hyper-viscosity ν_{hyp} is ad-hoc, and is included to prevent the formation of sharp gradients which are typical for self-focusing instabilities in 1D. The relation between Eqs. (13) and (6) may not be evident at first, and we explain the connection in the following. Equation (13) can be radially integrated once to obtain the up-gradient diffusion equation

$$\frac{\partial V_{ZF}}{\partial t} = -\frac{\partial}{\partial x}\left[\nu_{UG}\frac{\partial V_{ZF}}{\partial x}\right] - \mu V_{ZF} - \nu_{hyp}\frac{\partial^4 V_{ZF}}{\partial x^4}. \tag{16}$$

Equation (16) is identical to Eq. (6) in the reference case without RMPs ($\hat{b}_x = 0$), except that the last term on the r.h.s. of Eq. (16)—the hyperviscous dissipation term—is absent from Eq. (6). It may be possible to obtain this term from a closure of the Reynolds stress, but this is beyond the scope of this work.

2. 1D ZF-VF model

Taking into account RMP-induced field-line bending, we obtain—after some algebra—the following normalized 1D ZF-VF model:

$$\frac{\partial V_{ZF}}{\partial t} = -\hat{\nu}_{UG0}\frac{\partial}{\partial x}\left[\frac{\partial V_{ZF}}{\partial x} - \left(\frac{\partial V_{ZF}}{\partial x}\right)^3\right] - \hat{\nu}_{hyp}\frac{\partial^4 V_{ZF}}{\partial x^4} - \left[1 + \frac{1}{2}\frac{\hat{\mu}_{RMP}}{\hat{\mu}}\right]\hat{\mu}V_{ZF} + \frac{1}{2}\hat{D}_{\parallel}\hat{K}'_{\parallel}\hat{b}_x x\hat{\phi}, \tag{17}$$

$$\frac{\partial}{\partial t}\frac{\partial^2\hat{\phi}}{\partial x^2} = \hat{\nu}_{\perp}^{diss}\frac{\partial^4\hat{\phi}}{\partial x^4} + \hat{D}_{\parallel}\hat{K}'^2_{\parallel}x^2\hat{\phi} - \hat{D}_{\parallel}\hat{K}'_{\parallel}\hat{b}_x x V_{ZF}, \tag{18}$$

where time is normalized according to $t/\tau_s \to t$, with $\tau_s = (c_s/a)^{-1}$ the acoustic time. Space is normalized according to $x/\rho_s \to x$ with ρ_s the sound gyroradius. The electric potential associated with vortex-flow and zonal flows is normalized according to $e\hat{\phi}/(k_B T_e) \to \hat{\phi}$, and $e\phi_{zon}/(k_B T_e) \to \phi_{zon}$. The normalized zonal flows are then given by: $V_{ZF} = \partial\phi_{zon}/\partial x$. The normalized parameter $\hat{K}'_{\parallel}$ is defined as $\hat{K}'_{\parallel} = K_y\rho_s^2/L_s$.

B. Relation to the magnetic island-width

The ZF-VF system can be rewritten in the form

$$\frac{\partial V_{ZF}}{\partial t} + \hat{\mu}V_{ZF} + \hat{\nu}_{UG0}\frac{\partial}{\partial x}\left[\frac{\partial V_{ZF}}{\partial x} - \left(\frac{\partial V_{ZF}}{\partial x}\right)^3\right] + \hat{\nu}_{hyp}\frac{\partial^4 V_{ZF}}{\partial x^4} = -\hat{\mu}_{RMP}\left(V_{ZF} - \frac{x}{\hat{W}^2}\hat{\phi}\right), \tag{19}$$

$$\frac{\partial}{\partial t}\frac{\partial^2\hat{\phi}}{\partial x^2} - \hat{\nu}_{\perp}^{diss}\frac{\partial^4\hat{\phi}}{\partial x^4} = -\hat{\mu}_{RMP}\frac{x}{\hat{W}^2}\left(V_{ZF} - \frac{x}{\hat{W}^2}\hat{\phi}\right), \tag{20}$$

where $\hat{W}$ is the normalized island-width, given by

$$\hat{W} = \frac{W}{\rho_s} = \rho_s^{-1}\sqrt{\frac{L_s\hat{b}_x}{K_y}}. \tag{21}$$

Equation (20) is the charge balance analogue of—the small island limit of—the heat balance equation considered in Ref. 15. The mathematical form is similar, except that here, the source term depends on the profile of zonal flows. However, there is a major difference: the analysis in Ref. 15 relies on a crucial approximation, namely, the scale-separation between profile and helical perturbation. Note that in the case of Eq. (20), this approximation is invalid since zonal flows have a smaller radial scale than the vortex-flow pattern, as will be shown from the numerical results in Sec. III. The characteristic width of the vortex-flow pattern can be obtained, balancing the first and second terms on the r.h.s. of Eq. (18) the—unnormalized—width σ_ϕ of the vortex-flow pattern envelope, is given by

$$\sigma_\phi = \left[\frac{\rho_s^2\nu_{\perp}^{diss}L_s^2}{D_{\parallel}K_y^2}\right]^{1/6} \sim \nu_{ei}^{1/6}\rho_s^{1/3}L_s^{1/3}, \tag{22}$$

which has a similar scaling as the convective-cell width obtained in Ref. 18. We stress, however, that—in presence of RMPs—the width of the vortex-flow pattern in our simulations is enhanced compared to the unperturbed width Eq. (22).

III. NUMERICAL RESULTS

We implemented numerically the 1D ZF-VF model Eqs. (17) and (18) using Chebychev polynomials.[16] The spatiotemporal dynamics of zonal flows [Fig. 2(a)] and of the vortex-flow potential [Fig. 2(b)] are shown. Starting from random noise, the zonal flows first reach a saturated state, characterized by a certain amplitude and a large radial-scale through a sequence of mergers. Without RMPs, these mergers are halted due to the neoclassical zonal flow damping effect—the analogue of bottom drag in GeoFluid dynamics—which effectively sets the scale of zonal flows in this model. Then the RMPs are turned on at a time $t = 5$, and the system evolves towards a novel saturated state. In this novel state, zonal flow amplitude is lower—i.e., zonal flows are *damped*—and the ZF radial scale is smaller. Note the delay between application of RMPs at $t = 5$ and the time $t \simeq 5.5$ where the zonal flows reach a saturated state. We now turn to [Fig. 2(b)]. When RMPs are turned on, the associated VF potential grows. A

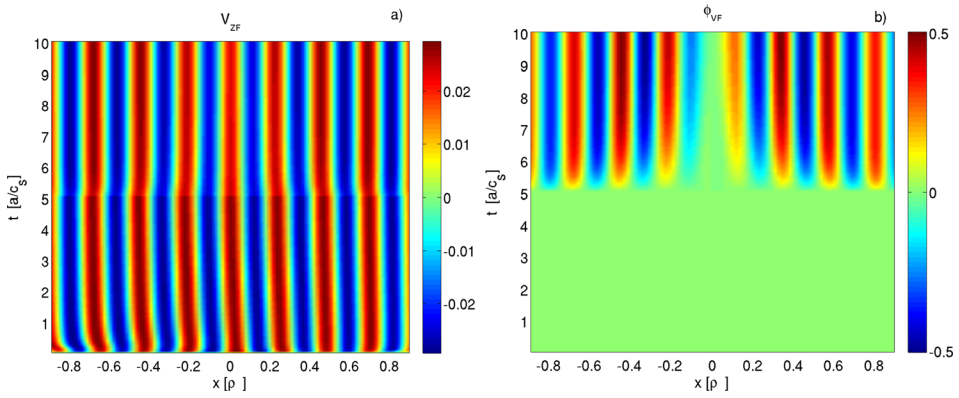

FIG. 2. Spatio-temporal dynamics of the 1D ZF-VF model: (a) x-t plot of zonal flows, and (b) vortex-flow electric potential. Parameters are $\hat{\nu}_{UG0} = 0.25$, $\hat{\nu}_{hyp} = 6.25 \times 10^{-5}$, $\hat{\nu}_{\perp}^{diss\prime} = 4 \times 10^{-3}$, $\hat{\mu} = 50$, $\hat{D}_{\parallel} = 1 \times 10^{8}$, $\hat{K}_{\parallel} = 1 \times 10^{-4}$, $\hat{b}_x = 2 \times 10^{-4}$ corresponding to $\hat{\mu}_{RMP}/\hat{\mu} = 0.5$ (c.f. Eq. (8)). The RMPs are turned on at $t = 5$. The associated normalized island-width is $\hat{W} = \sqrt{\hat{b}_x/\hat{K}_{\parallel}'} \simeq 1.41$.

close inspection reveals that zonal flow profile determines the fast radial-variation of the vortex flow pattern, while the slow radial variation is due to a combination of magnetic shear and dissipative effects (in our model viscous dissipation). In other words: zonal flows act as the *carrier-wave* for the vortex-flow pattern, whereas the vortex-flow *envelope* is set by spatial-resonance effects. Plotting the zonal flow energy $E_{ZF} = \int_{-L/2}^{L/2} {V_{ZF}}^2 dx$ [Fig. 3(a)] confirms that zonal flows are damped when RMPs are turned on at $t = 5$. We also show contours of the vortex-flow potential in the x-y plane at a given time $t = 10$, in the vicinity of the resonance surface [Fig. 3(b)]. We remind the reader that—in our notation—$y = r_s(\theta - \frac{N}{M}\varphi)$ is the helical angle. This figure clearly shows that the vortex-flow pattern exhibits *three scales*: the parallel modulation, the radial *fine-structure* due to zonal flows, and the radial envelope. The radial profiles of zonal flows and vortex-flow potential are also shown [Fig. 4]. Figure 5 shows that the Vortex-Flow energy at saturation scales as a power law vs. the RMP amplitude, with exponent $\alpha = 1.9$.

IV. DISCUSSION

Since zonal flows are a secondary instability, the vortex-flow pattern is a typical example of a *tertiary instability*. It is tempting to make an analogy with generalized Kelvin-Helmholtz modes;[17,18] however, unlike the K-H instability, the vortex-flow in our model relies crucially on the δB_r field to exist. In Ref. 18, the vortex-flow was also non-linearly driven, albeit directly by the Reynolds-stress. In our model, the vortex-flow is indirectly driven via RMP-induced coupling to zonal flows. Note that the electric potential associated to the vortex-flow pattern of our model is *in-phase* with the magnetic flux perturbation. Hence, it is different from the vortex-flow pattern associated to tearing-mode induced magnetic islands which is always in phase-quadrature ($\pi/2$ phase-shifted) with respect to the magnetic flux perturbation.

In Ref. 22, Rutherford presented, along with the well known nonlinear analysis, a quasilinear analysis—Eq. (22) in Ref. 22—showing that a tearing mode is stabilized by the non-linear damping of the tearing mode vortex-flow pattern—linearly driven by the equilibrium current gradient—varying as $\sin(K_y y)$, that is, $\pi/2$ phase shifted with respect to the magnetic flux perturbation. This nonlinear damping is due to what amounts to a zonal current. In Rutherford's quasilinear analysis, zonal flows are neglected, and the vortex-flow is driven linearly and damped nonlinearly. In our model, by taking into account zonal flows, we show that a different vortex-flow pattern varying as $\cos(K_y y)$ can be nonlinearly driven.

At this point, we would like to clarify the connection between our model—in which we work in the unperturbed coordinates—and the nonlinear tearing-mode theory described in island coordinates.[22] It can be shown that the vortex-flow that we describe in our theory is the non-axisymmetric component of the nonlinear flow of the tearing mode theory. One might ask then, what is the advantage of working in unperturbed coordinates? It is two-fold: (i) It allows to take into account the dynamical interaction between the zonal flows driven by microturbulence and the vortex-flow pattern and (ii) it allows to take into account neoclassical damping of the zonal flows which is the dominant damping mechanism for zonal flows in absence of magnetic perturbations.

An in-phase vortex-flow pattern has been observed in gyrokinetic turbulence simulations in presence of a static magnetic island.[19,20] In this reference, above a certain critical island-width, i.e., critical $\hat{b}_x$, the in-phase vortex-flow forms.

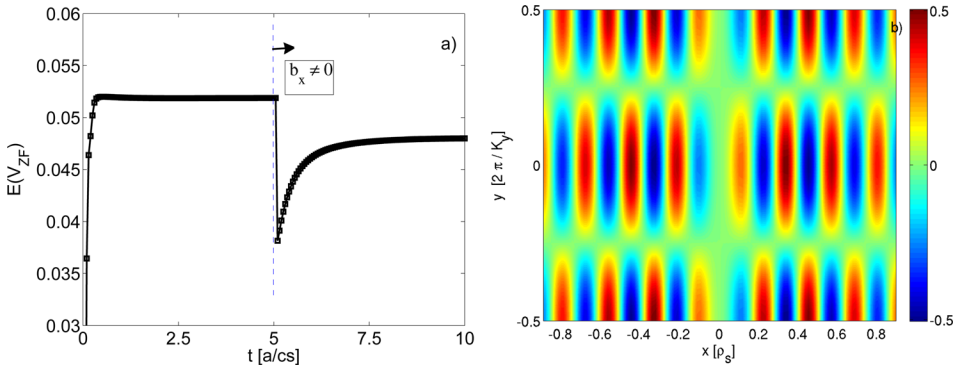

FIG. 3. RMPs damp zonal flows and drive vortex-flows: (a) Time series of the zonal flow energy, and (b) helical contours of the vortex-flow pattern at time $t = 10$, in the vicinity of the resonance surface $x = 0$. Parameters are the same as in Fig. 2.

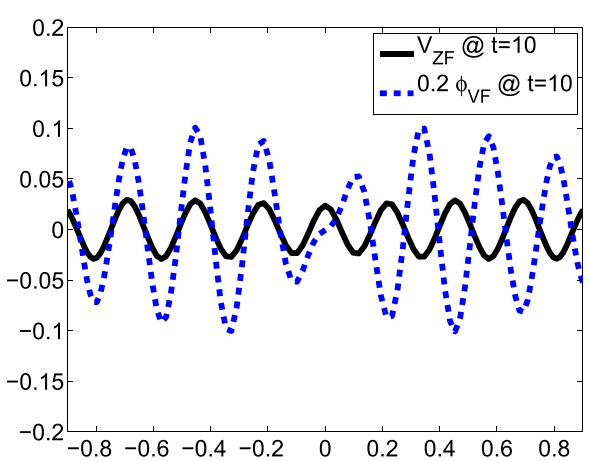

FIG. 4. Radial profiles of zonal flows V_{ZF} (full-line) and vortex-flow potential $\hat{\phi}$ (dashed-line) at a given time $t = 10$. Parameters are the same as in Fig. 2.

In these simulations, a density perturbation is also associated to the vortex-flow, hence the name "helical GAM" they use to refer to this new mode (although it is not induced by geodesic curvature). Note, however, that the vortex-flow in this reference has even parity, whereas in our model, the vortex-Flow has odd parity. In the gyrokinetic simulations of Ref. 19, due to flux-tube geometry, zonal flows ($m = 0, n = 0$) cannot be determined directly. However, in Fig. 7 of Ref. 19, the axisymmetric component of the total electric potential is clearly suppressed near the resonance surface—otherwise, the vortex could not form—as compared to a case without static island. This is indirect evidence of enhanced zonal flow damping near the resonance surface. Gyrokinetic simulations of Ref. 21, however, do not observe enhanced zonal flow damping. This could be due to screening effects due to the plasma response, which we do not consider in the present work. There are limitations to our model: (i) Our model is strictly only valid in the weak-coupling regime $\mu_{RMP}/\mu \ll 1$, where the zonal density perturbation—i.e., two fluid effect—is negligible. Since the neoclassical ZF damping is due to ion-ion collisions $\mu \sim \nu_{ii}$ and the RMP induced damping scales as $\mu_{RMP} \sim \hat{b}_x^2 \nu_{ei}^{-1}$, it means that our model is valid for small $\hat{b}_x$ or high collision frequency. (ii) The magnetic perturbation is assumed to be that generated by the RMP-coils; that is, we neglect the plasma response in our model and focus on RMP effect on nonlinear saturation of zonal flows. Taking into account the plasma response is beyond the scope of this article. (iii) The PDE that we use to model the evolution of zonal flows, although based on physical insight, is not derived from first principles. In particular, in our model, the dynamics of microturbulence is slaved to the dynamics of zonal flows. The self-consistent evolution of both, as in the 1D model of Ref. 23 (without RMPs) is important. However, in this reference, spatially-*random* zonal flows are assumed, whereas our analysis requires non-random, i.e., *coherent* zonal flows, since zonal flows are affected by the equilibrium magnetic shear due to the coupling to the vortex-flow pattern. As far as we know, there is no model, to date, treating coherent zonal flows and turbulence evolution self-consistently, so we focus here on zonal flows. Our approach is similar to that of Ref. 24, where a nonlinear equation describing zonal flows was derived. Hence, the effect of RMPs on the spatiotemporal characteristics of Limit-Cycle Oscillations (LCOs) cannot be addressed in our model. Experiments to address this effect, e.g., during a slow L-H transition, in the form of Ref. 25 and with RMP coils turned on, would be of great interest. (iv) Our model does not evolve density and temperature. The vortex-flow pattern can couple linearly to density and temperature to drive particle and heat transport convectively. Such a coupling is beyond the scope of this article, but heuristically, we expect the vortex-flow pattern—which varies like $\sim \cos(K_y y)$—to couple to a pressure pattern $\sim \sin(K_y y)$. Since mostly particle transport—and not heat transport—is observed in experiments, a related issue is how do the particle and heat channel decouple? We plan to investigate this somewhere else.

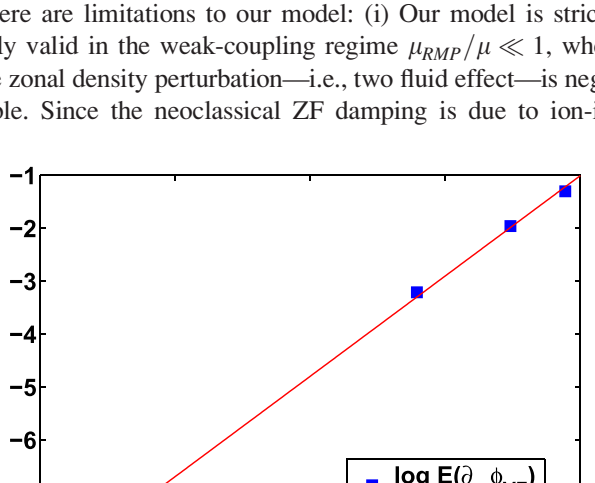

FIG. 5. Scaling-law of the vortex-flow energy vs. RMP amplitude $\hat{b}_x$, in the range $\hat{b}_x = 1 \times 10^{-5} - 3 \times 10^{-4}$. The obtained scaling is $E(\nabla\phi_{VF}) = \hat{b}_x^{\alpha}$, with $\alpha = 1.9$.

V. CONCLUSION

In this article, we showed that a long-lived vortex-flow pattern can be driven non-linearly by zonal flows, in presence of resonant magnetic perturbations, and we treated self-consistently the back-reaction of this vortex-flow pattern on zonal flows. This vortex-flow pattern grows by pumping energy out of zonal flows and is localized around the resonance surface. As zonal flows are turbulence-driven, this shows that turbulence plays a major role in the self-organization of helical states. The model predicts that the saturated vortex-flow energy $E = \int (\partial_r \phi_{VF})^2 dr$ scales with RMP amplitude as $E \sim \frac{\delta B_r}{B}^{\alpha}$ with $\alpha \simeq 1.9$. The associated enhancement in the particle transport—assuming the vortex flow pattern couples to density—has a resonant character. This additional transport could limit the pressure gradient in the pedestal below the ideal MHD threshold, and is therefore a possible candidate to explain ELM mitigation. A testable prediction is that the generation of this vortex-flow pattern is associated with a damping of zonal flows which occurs on a slow, transport timescale as opposed to the fast, Alfven-timescale penetration of RMPs. This implies a delay between RMP penetration and ELM mitigation. Such a delay has

been detected during ELM suppression experiments on the KSTAR tokamak,[26] and dubbed "secondary response." The scaling of this time-delay with respect to RMP amplitude and plasma parameters such as collisionality would be of valuable interest.

ACKNOWLEDGMENTS

The authors would like to thank Professor P. H. Diamond, K. J. Zhao, and W. A. Hornsby for useful discussions. This work was supported by R&D Program through National Fusion Research Institute (NFRI) funded by the Ministry of Science, ICT and Future Planning of the Republic of Korea (NFRI-EN1541-1).

[1]P. H. Diamond, S.-I. Itoh, K. Itoh, and T. S. Hahm, Plasma Phys. Controlled Fusion **47**, R35 (2005).
[2]T. E. Evans, M. E. Fenstermacher, R. A. Moyer, T. H. Osborne, J. G. Watkins, P. Gohil, I. Joseph, M. J. Schaffer, L. R. Baylor, M. Becoulet *et al.*, Nucl. Fusion **48**, 024002 (2008).
[3]Y. Liang, H. R. Koslowski, P. R. Thomas, E. Nardon, B. Alper, P. Andrew, Y. Andrew, G. Arnoux, Y. Baranov, M. Becoulet *et al.*, Phys. Rev. Lett. **98**, 265004 (2007).
[4]W. Suttrop, T. Eich, J. C. Fuchs, S. Gunter, A. Janzer, A. Herrmann, A. Kallenbach, P. T. Lang, T. Lunt, M. Maraschek *et al.*, Phys. Rev. Lett. **106**, 225004 (2011).
[5]Y. M. Jeon, J. K. Park, S. W. Yoon, W. H. Ko, S. G. Lee, K. D. Lee, G. S. Yun, Y. U. Nam, W. C. Kim, J. G. Kwak *et al.*, Phys. Rev. Lett. **109**, 035004 (2012).
[6]G. R. McKee, Z. Yan, C. Holland, R. J. Buttery, T. E. Evans, R. A. Moyer, S. Mordijck, R. Nazikian, T. L. Rhodes, O. Schmitz *et al.*, Nucl. Fusion **53**, 113011 (2013).
[7]M. Leconte and P. H. Diamond, Phys. Plasmas **19**, 055903 (2012).
[8]P. Beyer, X. Garbet, S. Benkadda, P. Ghendrih, and Y. Sarazin, Plasma Phys. Controlled Fusion **44**, 2167 (2002).
[9]Y. Xu, D. Carralero, C. Hidalgo, S. Jachmich, P. Manz, E. Martines, B. van Milligen, M. A. Pedrosa, M. Ramisch, I. Shesterikov *et al.*, Nucl. Fusion **51**, 063020 (2011).
[10]M. Leconte, P. Beyer, X. Garbet, and S. Benkadda, Nucl. Fusion **50**, 054008 (2010).
[11]N. Vianello, C. Rea, M. Agostini, R. Cavazzana, G. Ciaccio, G. de Masi, E. Martines, A. Mazzi, B. Momo, G. Spizzo *et al.*, Plasma Phys. Controlled Fusion **57**, 014027 (2015).
[12]F. A. Marcus, P. Beyer, G. Fuhr, A. Monnier, and S. Benkadda, Phys. Plasmas **21**, 082502 (2014).
[13]M. Leconte, P. H. Diamond, and Y. Xu, Nucl. Fusion **54**, 013004 (2014).
[14]A. J. Manfroi and W. R. Young, J. Atmos. Sci. **56**, 784 (1999).
[15]R. Fitzpatrick, Phys. Plasmas **2**, 825 (1995).
[16]R. Peyret, *Spectral Methods for Incompressible Viscous Flow* (Springer, 2000).
[17]B. N. Rogers, W. Dorland, and M. Kotschenreuther, Phys. Rev. Lett. **85**, 5336 (2000).
[18]C. McDevitt and P. H. Diamond, Phys. Plasmas **14**, 112306 (2007).
[19]W. A. Hornsby, A. G. Peeters, A. P. Snodin, F. J. Casson, Y. Camenen, G. Szepesi, M. Siccinio, and E. Poli, Phys. Plasmas **17**, 092301 (2010).
[20]W. A. Hornsby, A. G. Peeters, M. Siccinio, and E. Poli, Phys. Plasmas **19**, 032308 (2012).
[21]R. E. Waltz and F. L. Waelbroeck, Phys. Plasmas **19**, 032508 (2012).
[22]P. H. Rutherford, Phys. Fluids **16**, 1903 (1973).
[23]K. Miki, P. H. Diamond, O. Gurcan, G. R. Tynan, T. Estrada, L. Schmitz, and G. S. Xu, Phys. Plasmas **19**, 092306 (2012).
[24]M. N. Rosenbluth and V. D. Shapiro, Phys. Plasmas **1**, 222 (1994).
[25]L. Schmitz, L. Zeng, T. L. Rhodes, J. C. Hillesheim, E. J. Doyle, R. J. Groebner, W. A. Peebles, K. H. Burrell, and G. Wang, Phys. Rev. Lett. **108**, 155002 (2012).
[26]Y. M. Jeon, J. K. Park, T. E. Evans, G. Park, Y. C. Ghim, H. Han, W. H. Ko, Y. U. Nam, K. D. Lee, S. G. Lee *et al.*, "Successful ELM suppressions in a wide range of q_{95} using low n RMPs in KSTAR and its understanding as a secondary effect of RMP," in 25th IAEA Fusion Energy Conference, St Petersburg, Russia, 2014, Paper No. EX/1-5.